OPTIMIZATION OF SELF-ORGANIZED GROWTH OF NANOPOROUS ANODIC ALUMINA TEMPLATES FOR CAPACITOR APPLICATION

LEDNICKÝ Tomáš, MOZALEV Alexander

Central European Institute of Technology (CEITEC), Brno University of Technology, Brno, Czech Republic

Abstract

High-voltage nanoporous anodic films grown on aluminium in certain organic electrolytes are of increasing interest for potential applications as nanotemplates to electrical capacitors and, more generally, as models for investigating self-organized growth of anodic oxides at the frontier conditions. The major difficulty associated with this technology is that the process of pore nucleation and growth over a large-area aluminium substrate needs optimization and adaptation to the specific technological conditions applied to aluminium substrates as the surface finishing pre-treatments. In this work we have studied the impact of important pre-treatment technologies for Al foils, such as high temperature annealing and electrochemical polishing, on the pore nucleation and growth during galvanostatic formation of nanoporous anodic alumina templates in aqueous solutions of citric acid. It was revealed that the self-organized pore nucleation and growth is strictly dependent upon the anodizing setup, anodizing variables, surface morphology and crystalline structure of aluminium foils, which are additionally affected by the conditions of vacuum annealing and electropolishing pre-treatments. The findings are useful for growing well-ordered nanopores for non-lithographic formation of metal and metal-oxide nanostructures for advanced capacitor application.

Keywords: **anodizing, citric acid, porous anodic alumina, nanostructure, capacitor**

1. INTRODUCTION

Anodic oxidation of aluminium and the growth of porous anodic alumina (PAA) films in acidic electrolytes have been intensively investigated over the last few decades focusing primarily on mechanical toughness and chemical stability of aluminium. In the recent years, with the development of nanotechnology, the new wave of interest has arisen towards application of PAA for forming a range of self-organized nanoporous templates in a facile and cost-effective way. PAA films having self-ordered versatile structure have also been proposed as support substrates for increasing the surface area of active layers employed in chemical sensors, electrical capacitors, rechargeable batteries, solar cell etc. [1-5]. Formation of PAA in *citric acid* at high anodizing potentials, often exceeding 300 V, gives the oxide cells approaching the micrometer range [6, 7]. Nowadays, study and development of such large nanostructures are of importance for the development of advanced non-lithographic microfabrication techniques. However, a uniform growth of self-organized PAA films in citric acid has been a challenge due to the lack of knowledge about the right combination of technological, electrical and electrolytic conditions for pore nucleation and growth in this acid.

In the present work, we have studied the effects of aluminium structure and morphology on the anodizing behaviour of aluminium and the growth of alumina pores in 0.05 M citric acid and the effect of annealing and electropolishing pre-treatments. Further, through optimization of self-organized growth of the nanoporous anodic alumina films we have demonstrated potential application of citric-acid-made PAA as a template for nanostructuring metals and dielectrics for advanced capacitor applications.

2. MATERIALS AND METHODS

2.1. Aluminium anodization in citric acid

An aluminium foil of 99.999 % purity and 100 μm thickness (Goodfellow) was used as the initial material. The foil was cut into square pieces of about 2 cm × 2 cm. Four types of aluminium structures were obtained by combining various treatments: as rolled, annealed, electro-chemically polished, and a combination of annealed and electrochemically polished samples. All samples were first washed in ethanol, acetone and distilled water. Then, part of them was annealed in a vacuum at 550 °C for 5 h to allow the material to relax and recrystallize. The electrochemical polishing was done in a mixture of perchloric acid and ethanol (1:4 *v*:*v*) at 2–5 °C at 20 V for 1 min. The samples were then anodized in 0.05 M citric acid (Sigma-Aldrich) aqueous solution at constant current densities of 1 to 10 $mA \cdot cm^{-2}$ at starting electrolyte temperature of 22.5 °C ± 0.5 °C. The anodization was performed in a specially designed PTFE two-electrode cell having a 10-mm protecting ring as described elsewhere [9]. The potential-time responses during galvanostatic anodizing of aluminium foils were recorded until a steady-state pore growth occurred, which is associated in the classical model with a relatively constant potential on the anodizing curves [10]. After anodizing, the oxide film was selectively removed from each sample by immersion in a hot (approximately 65 °C) water solution of 0.2 M chromium trioxide and 0.42 M phosphoric acid for 1.5 h. The treated, anodized (anodic alumina) and etched (residual aluminium substrate) samples were observed in a Tescan Mira II field emission scanning electron microscope (SEM).

2.2. Nanostructured substrate preparation

For nanostructured template preparation, the as-rolled aluminium foil of 1 cm × 3 cm size was used. A PAA film was prepared by a two-step anodization technique [4] in 0.6 M citric acid aqueous solution. The first anodization was conducted with the initial potential sweep of 0.5 $V \cdot s^{-1}$ up to 300 V. After reaching the potential limit, the sample was anodized potentiostatically for 20 h in a stirred electrolyte at temperature of 23.5 °C. Then, the oxide layer was dissolved in the selective etchant at 70 °C for 1.5 h. The second anodization was conducted under the same anodizing conditions but it lasted only 5 min. The pore widening was performed in the same selective etchant of alumina at 60 °C for 27 min, after which the sample was immediately washed in distilled water.

3. RESULTS AND DISCUSSION

3.1. Aluminium anodization in citric acid

Fig. 1 shows potential-time responses for anodizing the as-rolled, annealed and polished aluminium foils at various formation current densities (as measured) in 0.05 M citric acid. As seen, the anodizing behaviour of the as-rolled samples differs substantially from a classical model. The usual galvanostatic anodizing in acidic electrolytes is associated with the increase in peak and steady-state potentials with increasing the current density [11]. This behaviour is demonstrated in the inset graph (**Fig. 1**) of galvanostatic anodizing of aluminium foil in phosphoric acid. The increase of current density normally leads to thickening the alumina barrier layer, enlarging the oxide cells and increasing the pore diameter; these all being associated with increasing the anodizing potential.

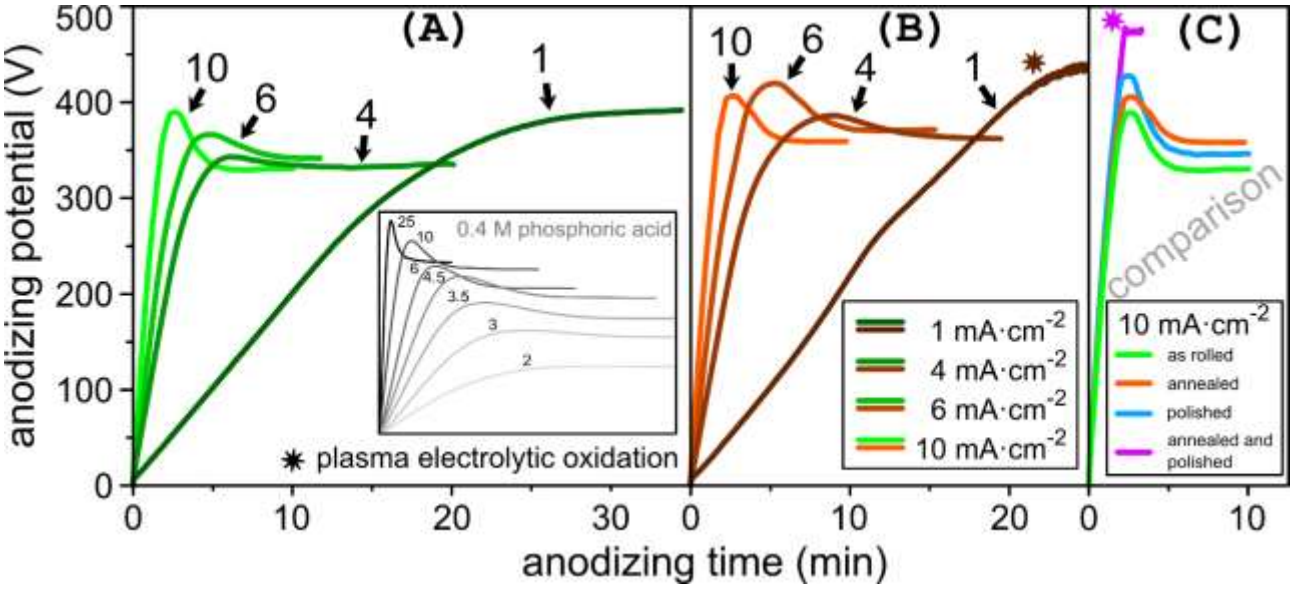

Fig. 1 Potential-time responses of (A) as rolled, (B) vacuum annealed aluminium foils during galvanostatic anodizing in 0.05 M citric acid. (C) shows the comparison of galvanostatic anodization at 10 mA·cm^{-2} for various foils. The inset shows a classical galvanostatic anodizing behaviour of aluminium foil in 0.4 M phosphoric acid acid.

During the galvanostatic anodization, the first linear rise of the potential is related to the growth of a compact anodic layer. When critical conditions are reached, the pore formation occurs and the potential begins to retard, which indicate the transformation of the compact oxide film into a porous anodic layer. After a period of the pore nucleation and competition, the film growth turns usually into the steady-state regime which is characterized by a relative constant potential after the initial peak. The steady-state regime in acidic electrolytes is commonly accompanied by the porous layer growth over the whole aluminium surface area.

Contrary to the classical model [8], anodizing in the citric acid shows the tendency of increasing potential with decreasing the current density. The formation potential increased enormously at the lowest current density while the highest current resulted in the lowest potential. The same unexpected tendency was observed also for the annealed samples, additionally to the systematic rise in the formation potential. The rise of formation potential leaded at the lowest current density (1 mA·cm^{-2}) to plasma electrolytic oxidation (PEO), which is characterized by intense generation of spark discharges and gas evolution. Furthermore, for the polished samples, except the 10 mA·cm^{-2} case (**Fig. 1C**), anodizing at other current densities resulted in undesirable PEO, which prevented pore growth. Moreover, PEO appeared to be the only outcome of the annealed and polished sample anodizing at the selected current densities (shown only for 10 mA·cm^{-2} in **Fig. 1C**).

This counterintuitive behaviour can be explained through a detailed analysis of the SEM images (some examples of the as rolled foil anodized images are shown in **Fig. 2**) demonstrating the as anodized porous alumina layer and the development of concave imprints of the alumina cells in the residual aluminium. At the lowest current density (1 mA·cm^{-2}), the pore nucleation as well as pore growth are greatly hindered, resulting in the large compactly anodized (pore-free) area. With increasing the current density the pores nucleate over the whole sample surface. This phenomenon is shown in detail on the graph of pore-free area *vs.* current density in **Fig. 2C**. We suggest that the main reason for this phenomenon is the hindered field-assisted dissolution caused by the low anodizing current density. In the case of weak and diluted citric acid, the applied current density (1 mA·cm^{-2}) is not sufficient to achieve critical conditions for pore formation over the whole surface. Thus, pores nucleate and growth only in the area where the local current density is sufficient to stimulate oxide dissolution. The role of field-assisted dissolution can be further explained by comparing the anodizing behaviour of the differently treated aluminium foils (**Fig. 1C**).

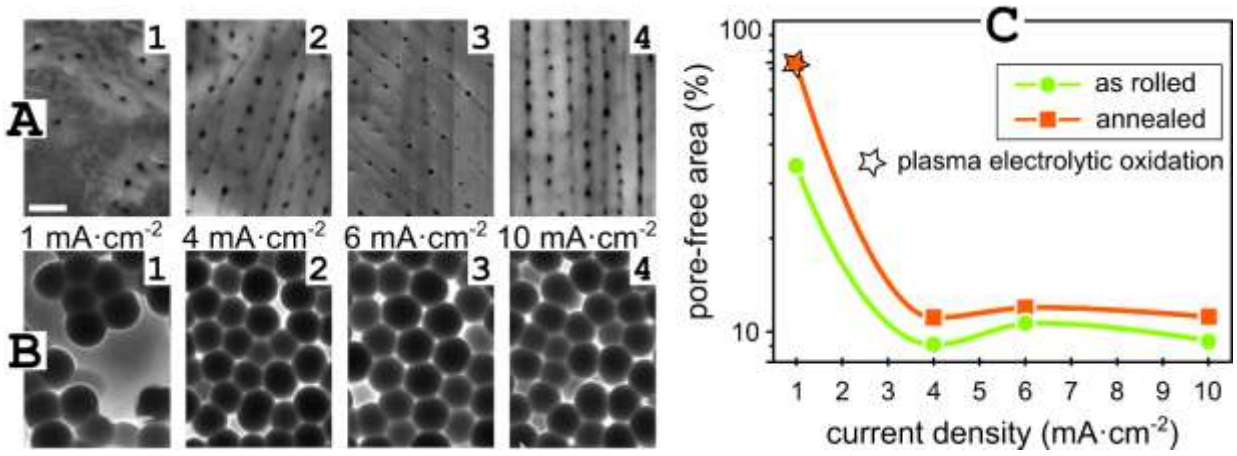

Fig. 2 SEM images of the as-rolled foils anodized as in **Fig. 1A** before (row A) and after (row B) selective alumina dissolution. The graph (C) shows the pore-free area vs. anodized current density curves (as measured) for the as-rolled and annealed foils anodized as in **Fig. 1A-B**. The scale bar is 3 μm.

The annealed foils exhibited the potential increase in the nucleation and steady-state stage. We suggest that the origin of this increase is the enhanced chemical stability of the annealed foils leading to the suppressed field-assisted dissolution. The anodizing responses of the annealed foils were similar to those of the as-rolled foils in the initial stage, representing the nucleation of pores. However, the peak representing pore competition was weak and the steady-state potential was considerably higher. This reveals that pore growth is less favorable compared with the as-rolled foils, leading to the smaller pore population and larger cell size (illustrated in **Fig. 2C**).

In case of the polished foils, the main potential increase during the initial stage is the consequence of smoother aluminium surface, resulting in the decrease in pore nucleation sites (micro-/nano- defects like cracks, pits, etc.), which may work as preferable centers enhancing the effect of field-assisted dissolution. Thus, during the initial stage, the pore nucleation is mostly hindered and the compact oxide layer growth is preferred.

3.2. Nanostructured substrate preparation

The findings show that the growth of a uniform porous layer depends on the aluminium surface morphology as well as on the anodizing conditions. Thus, for uniform growth, the as-rolled aluminium foil and 0.6 M citric acid were selected to enhance the oxide dissolution ability of the electrolyte. The main feature of the alumina templates for application in capacitor fabrication is the enlargement of active surface area by 3-D nanostructuring and thus increasing the capacitance per apparent surface area compared with a planar capacitor having the same thickness of dielectric on a smooth substrate.

Furthermore, a low aspect ratio of the pores is more favorable for making the anodizing technology compatible with standard microfabrication processes. The PAA prepared by the two-step anodization method to achieve homogeneous and well-ordered pores is shown in **Fig. 3A**. Subsequent pore widening was applied to enlarge pore diameters from 150 nm up to 600 nm. As a result, a porous anodic template (shown in **Fig. 3B**) with the thickness of 800 nm and the pore aspect ratio of 1.5 was obtained.

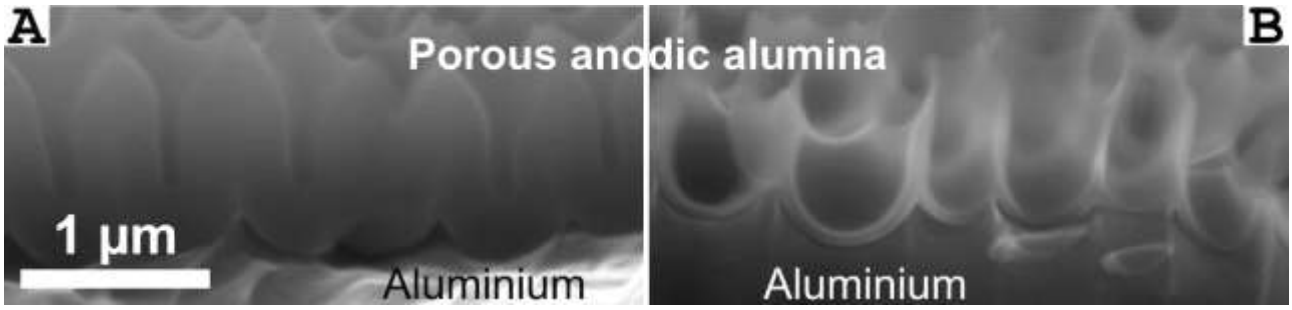

Fig. 3 SEM cross-section images of porous anodic alumina formed in 0.6 M citric acid at 300 V by the two-step anodization, (A) as anodized, (B) after pore widening.

SUMMARY AND CONCLUSIONS

The findings of this work revealed the abnormal anodizing and pore formation behaviour of aluminium in the diluted citric acid electrolyte. The decrease in measured current density results in increasing the formation potential, cell sizes and in reducing substantially the pore population density. This phenomenon is additionally influenced by the high temperature annealing and electrochemical polishing. We proposed a straight-forward explanation based on the field-assisted dissolution which is in both cases inhibited by the material morphology or structural changes in comparison with the untreated foils. At the specific anodizing conditions, it is possible to achieve, for the first time, the growth of a hybrid anodic film composed of a compact layer and a porous alumina layer. The findings are useful for forming well-ordered alumina nanopores without external techniques for non-lithographic fabrication of metal and metal-oxide nanostructures for advanced electrical and optical applications.

The proposed approach delivers new possibilities and challenges into the vast field of aluminium anodization and utilization of anodizing techniques [12-14]. The present results are of vast importance for the development of aluminium anodizing processes for use in future nanodevices, where PAA films can be utilized as templates or supporting substrates, especially, for novel thin film capacitors [15] with 3-D nanostructuring, aiming to enlarge the film active area and increase the final device capacitance without raising the original device dimensions. This research is in progress now, the results to be reported in due course.

ACKNOWLEDGEMENTS

Research leading to these results was supported in part by a grant from the Czech Science Foundation (GA ČR) no. 14-29531S and in part by a project of CEITEC no. STI-J-15-2886

REFERENCES

[1] SOLOVEI D., HUBÁLEK J. and MOZALEV A., The growth and dielectric properties of porous-anodic-alumina-supported nanostructured Ta_2O_5/Ta films, 63rd Annual Meeting of the International Society of Electrochemistry (ISE2012), Prague, 2012, pp. 1.

[2] LEE W. and PARK S.-J., Porous Anodic Aluminum Oxide: Anodization and Templated Synthesis of Functional Nanostructures, Chemical Reviews, Vol. 114, No. 15, 2014, pp. 7487-7556.

[3] KHATKO V., MOZALEV A., GOROKH G., SOLOVEI D., GUIRADO F., LLOBET E. and CORREIG X., Evolution of Surface Morphology, Crystallite Size, and Texture of WO_3 Layers Sputtered onto Si-Supported Nanoporous Alumina Templates, Journal of The Electrochemical Society, Vol. 155, No. 7, 2008, pp. K116-K123.

[4] SULKA G. D., Highly Ordered Anodic Porous Alumina Formation by Self-Organized Anodizing, Nanostructured Materials in Electrochemistry, Wiley-VCH Verlag GmbH & Co. KGaA, 2008, pp. 1-116.

[5] BLACKMAN C. S., CORREIG X., KATKO V., MOZALEV A., PARKIN I. P., ALCUBILLA R. and TRIFONOV T., Templated growth of tungsten oxide micro/nanostructures using aerosol assisted chemical vapour deposition, Materials Letters, Vol. 62, No. 30, 2008, pp. 4582-4584.

[6] MOZALEV A., MOZALEVA I., SAKAIRI M. and TAKAHASHI H., Anodic film growth on Al layers and Ta–Al metal bilayers in citric acid electrolytes, Electrochimica Acta, Vol. 50, No. 25–26, 2005, pp. 5065-5075.

[7] YANG J., HUANG H., LIN Q., LU L., CHEN X., YANG L., ZHU X., FAN Z., SONG Y. and LI D., Morphology defects guided pore initiation during the formation of porous anodic alumina, ACS Applied Materials and Interfaces, Vol. 6, No. 4, 2014, pp. 2285-2291.

[8] THOMPSON G. E., Porous anodic alumina: fabrication, characterization and applications, Thin Solid Films, Vol. 297, No. 1–2, 1997, pp. 192-201.

[9] MOZALEV A., CALAVIA R., VÁZQUEZ R. M., GRÀCIA I., CANÉ C., CORREIG X., VILANOVA X., GISPERT-GUIRADO F., HUBÁLEK J. and LLOBET E., MEMS-microhotplate-based hydrogen gas sensor utilizing the nanostructured porous-anodic-alumina-supported WO_3 active layer, International Journal of Hydrogen Energy, Vol. 38, No. 19, 2013, pp. 8011-8021.

[10] SURGANOV V. F. and GOROKH G. G., Anodic oxide cellular structure formation on aluminum films in tartaric acid electrolyte, Materials Letters, Vol. 17, No. 3, 1993, pp. 121-124.

[11] WOOD G. C., Porous anodic films on aluminum, in D. J. W, ed., Marcel Dekker Inc., New York, 1973, pp. 167-279.

[12] VERGARA A., CALAVIA R., VÁZQUEZ R. M., MOZALEV A., ABDELGHANI A., HUERTA R., HINES E. H. and LLOBET E., Multifrequency interrogation of nanostructured gas sensor arrays: A tool for analyzing response kinetics, Analytical Chemistry, Vol. 84, No. 17, 2012, pp. 7502-7510.

[13] MOZALEV A., VÁZQUEZ R. M., BITTENCOURT C., COSSEMENT D., GISPERT-GUIRADO F., LLOBET E. and HABAZAKI H., Formation–structure–properties of niobium-oxide nanocolumn arrays via self-organized anodization of sputter-deposited aluminum-on-niobium layers, Journal of Materials Chemistry C, Vol. 2, No. 24, 2014, pp. 4847-4847.

[14] MOZALEV A., HABAZAKI H. and HUBÁLEK J., The superhydrophobic properties of self-organized microstructured surfaces derived from anodically oxidized Al/Nb and Al/Ta metal layers, Electrochimica Acta, Vol. 82, 2012, pp. 90-97.

[15] MOZALEV A., SAKAIRI M., TAKAHASHI H., HABAZAKI H. and HUBÁLEK J., Nanostructured anodic-alumina-based dielectrics for high-frequency integral capacitors, Thin Solid Films, Vol. 550, 2014, pp. 486-494.